Electronic Supplementary Information

Recycling spent $LiNi_{1-x-y}Co_xMn_yO_2$ cathodes to efficient catalysts for oxygen evolution reaction

Mingfei Chen,[a] Yixin Zhou,[a] Li Wang,[a, b] Gang Xue,[a, b] Jiashuo Guo,[a] and Yaping Wang*[a, b]

[a] School of Materials Science and Engineering, Hebei University of Technology, Tianjin, 300130, China.

[b] Key Laboratory of Special Functional Materials for Ecological Environment and Information (Hebei University of Technology), Ministry of Education, Tianjin, 300130, China.

Email: wangyaping@hebut.edu.cn (Y. Wang)

Experimental Section

Raw Materials: The spent lithium-ion batteries with different $LiNi_{1-x-y}Co_xMn_yO_2$ (NCM) cathodes were first soaked in a 10 wt.% NaCl solution, followed by manual disassembling into the cathode, anode, and separator. Then, the positive electrode was treated at 450 °C for 3 h in the air to remove the binder, and the black powders of the NCM cathode were collected.

Preparation of NCM Hydroxide Catalyst: First, 4.19 g of choline chloride (CHCL) and 6.42 g of citric acid (CA) were dispersed into the mixed solvent of ethylene glycol (33 mL) and water (11 mL) by string to obtain the DES solution. Then, 0.60 g of as-prepared NCM cathode raw material was added into the above DES solution under magnetic stirring for 2 h at 90 °C and filtered to obtain a precursor solution (Solution A). 2.52 g of oxalic acid was dispersed in the mixed solvent of ethylene glycol (12 mL) and water (4 mL) to form Solution B. Then, Solution B was slowly added to Solution A at room temperature with continuous stirring to the suspension liquid. The above mixture was transferred into a 100 mL Teflon-lined stainless-steel autoclave, which was sealed and heated in an electronic oven at 180 °C for 12 h. After cooling down to room temperature, the precipitate was filtered and washed several times with deionized water and dried at 60 °C for 12 h to obtain NCM oxalate (NCM-OA). Subsequently, 0.2 g of NCM-OA was dispersed in 50 mL of 1 M KOH aqueous solution by ultrasonic for 5 min at room temperature. After filtered and washed several times with deionized water, the NCM hydroxide (NCM-OH) catalyst is prepared. Here we denote the NCM-OH catalyst as the sample prepared from spent $LiNi_{0.33}Co_{0.33}Mn_{0.33}O_2$. The samples

made from spent $LiNi_{0.9}Co_{0.05}Mn_{0.05}O_2$, $LiNi_{0.8}Co_{0.1}Mn_{0.1}O_2$, $LiNi_{0.6}Co_{0.1}Mn_{0.3}O_2$, and $LiNi_{0.5}Co_{0.2}Mn_{0.3}O_2$ were named NCM-OH-955, NCM-OH-811, NCM-OH-613, and NCM-OH-523, respectively.

For comparison, the hydroxides with single, binary, or ternary metal elements were prepared using nickel chloride hexahydrate, cobalt chloride hexahydrate, or (and) manganese (II) chloride tetrahydrate with a total amount of 6 mmol as the raw metal sources. The obtained samples were $Ni(OH)_2$, $Co(OH)_2$, $Mn(OH)_2$, $Ni_{0.5}Co_{0.5}(OH)_2$, $Ni_{0.5}Mn_{0.5}(OH)_2$, and $Co_{0.5}Mn_{0.5}(OH)_2$, and $Ni_{0.33}Co_{0.33}Mn_{0.33}(OH)_2$ accordingly.

Material Characterization: The morphology and element distribution of the samples were characterized by scanning electron microscopy (SEM, JEOL 7610F) and transmission electron microscopy (TEM, JEM 2100F) combined with energy-dispersive X-ray spectroscopy. The X-ray diffractions were collected by an X-ray diffractometer (Rigaku smart lab, 4 KW) at room temperature with Cu-Kα radiation (λ = 0.154 nm) in a scanning range of 5° to 80° (2θ). The compositional analysis of the samples was carried out by XPS (ESCALAB250Xi). Raman spectroscopy measurements were carried out at room temperature using a Raman spectrometer (LabRAM HR Evolution, HORIBA) at 532 nm excitation. Fourier-transform infrared (FT-IR) spectra were obtained using an infrared spectrometer (VERTEX 80/80 V). Brunauer-Emmett-Teller (BET) adsorption isotherm obtained from Autosorb iQ2-C-TPX was used to calculate the specific surface area and pore size. The metallic element contents were determined by inductively coupled plasma-mass spectrometry (PRODIGY XP).

Electrochemical Measurements: The obtained catalytic materials, acetylene black and polyvinylidene fluoride (PVDF) in a weight ratio of 80:10:10 were dispersed in N-methyl-2-pyrrolidone (NMP) solution to form a slurry, which was coated on a piece of hydrophilic carbon cloth (1*1 cm^2) and dried in a vacuum oven at 60 °C for 10 h. The mass loading of catalytic materials is approximately 0.53 mg cm^{-2}. The electrochemical tests were carried out on an electrochemical workstation (CHI660E, Shanghai) at room temperature using a three-electrode system with a graphite rod (d = 6 mm) counter electrode and a Hg/HgO (1 M KOH) reference electrode in 1 M KOH aqueous solution as the electrolyte. All potentials in this study were calibrated to reversible hydrogen electrode (RHE) potentials according to the following equation:

$$E_{vsRHE} = E_{Hg/HgO} + 0.098 + 0.059 \times pH$$

Linear sweep voltammetry (LSV) was carried out in 1 M KOH solution with a scan rate of 5 mV s^{-1}. Staircase voltammetry (SCV) was carried out with an SCV jump potential of 0.05 V, and each step was held for 200 s. Tafel slopes were calculated from the corresponding SCV curves. The current density-time (*i*-*t*) curves of OER activity were measured at 1.51 V. The long-term stability test was evaluated by chronopotentiometry at a constant current density of 10 mA cm^{-2} for 100 h. Electrochemical impedance spectroscopy (EIS) was recorded with an amplitude of 5 mV at a frequency range from 0.1 to 100 kHz. Electrochemical-specific surface area (ECSA) was tested by cyclic voltammetry (CV) at different scan rates from 10 to 100 mV s^{-1} at 0.93-1.03 V (vs. RHE).

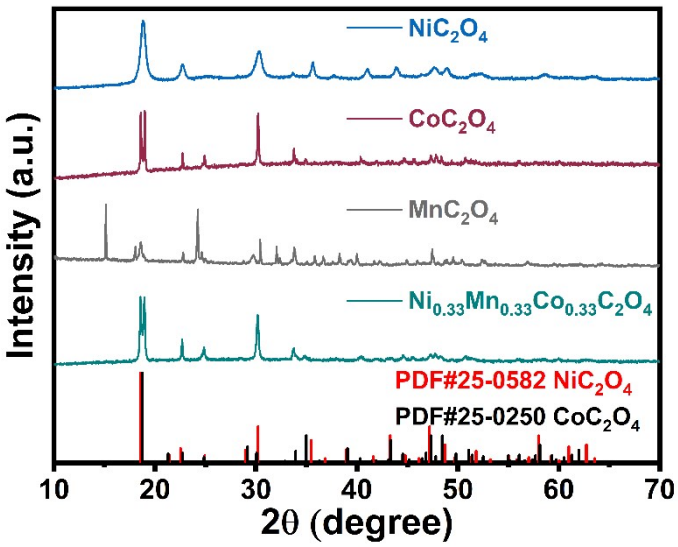

Fig. S1 The XRD patterns of NiC_2O_4, CoC_2O_4, MnC_2O_4, and $Ni_{0.33}Co_{0.33}Mn_{0.33}C_2O_4$ samples.

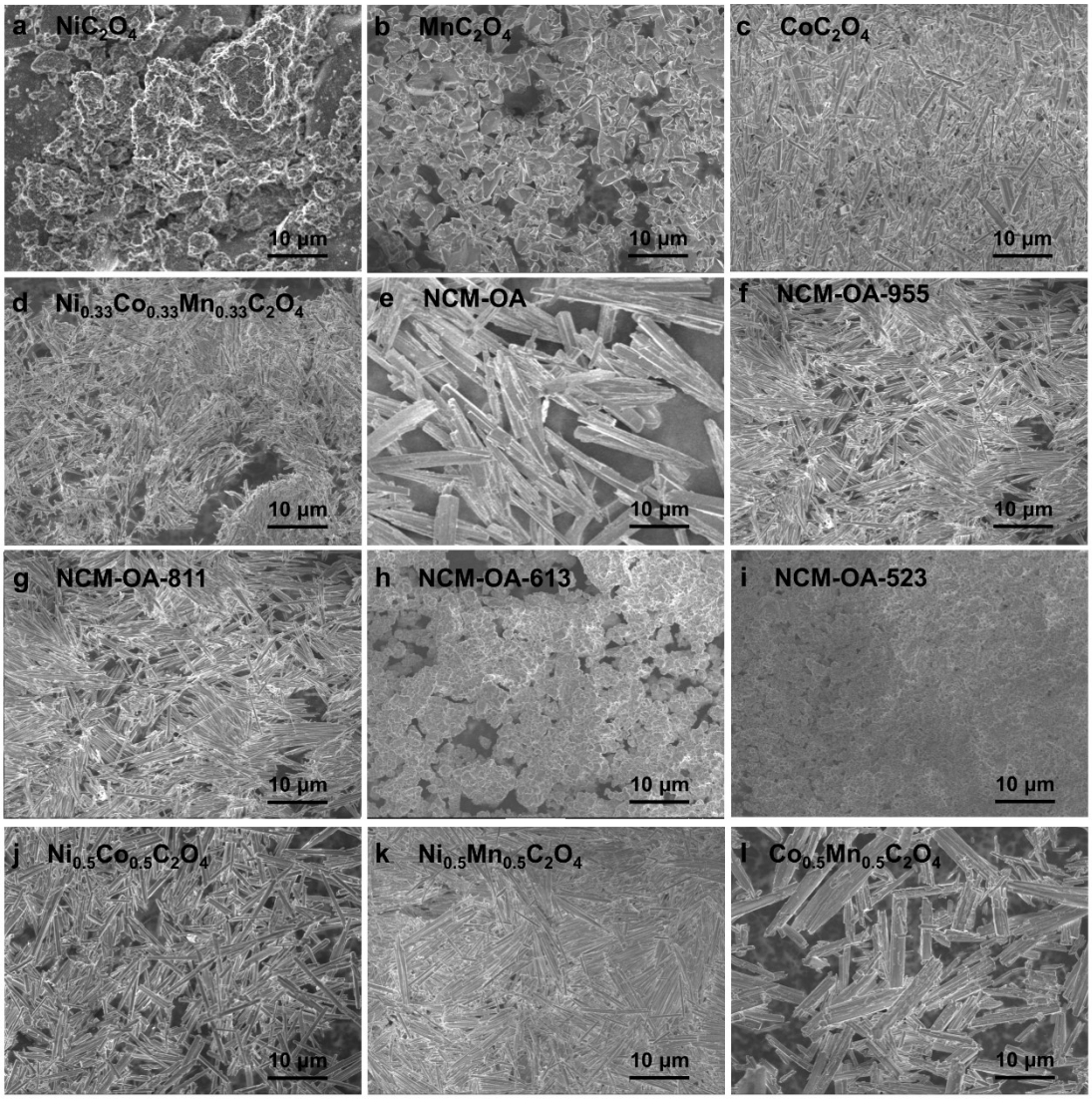

Fig. S2 SEM images of (a) NiC_2O_4, (b) MnC_2O_4, (c) CoC_2O_4, (d) $Ni_{0.33}Co_{0.33}Mn_{0.33}C_2O_4$, (e) NCM-OA, (f) NCM-OA-955, (g) NCM-OA-811, (h) NCM-OA-613, (i) NCM-OA-523, (j) $Ni_{0.5}Co_{0.5}C_2O_4$, (k) $Ni_{0.5}Mn_{0.5}C_2O_4$, and (l) $Co_{0.5}Mn_{0.5}C_2O_4$.

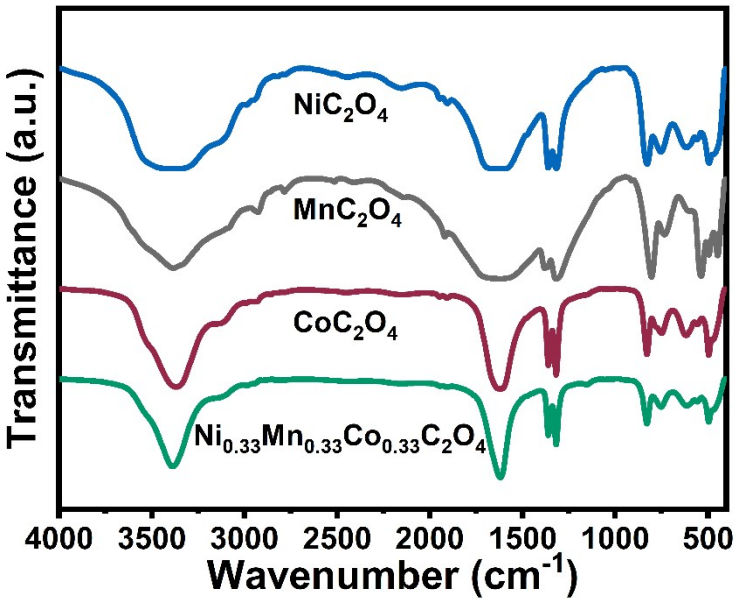

Fig. S3 The FT-IR spectra of NiC_2O_4, MnC_2O_4, CoC_2O_4, and $Ni_{0.33}Co_{0.33}Mn_{0.33}C_2O_4$.

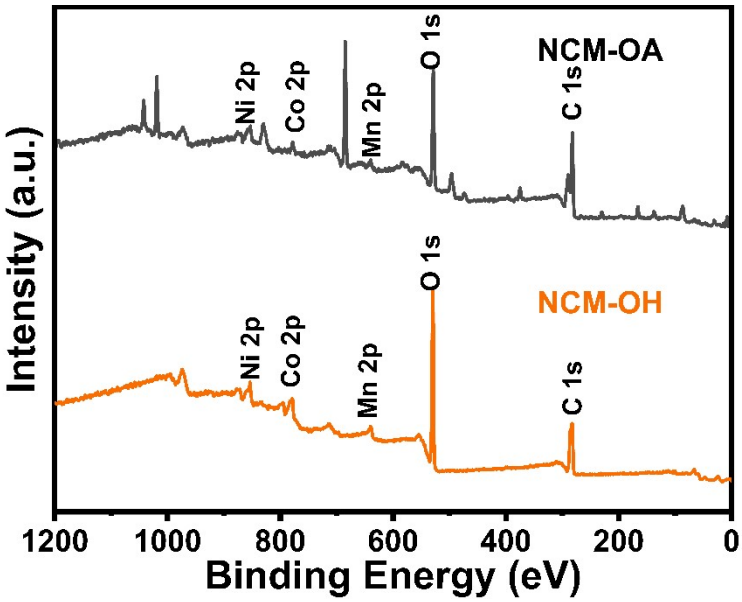

Fig. S4 The survey XPS spectra of NCM-OA and NCM-OH.

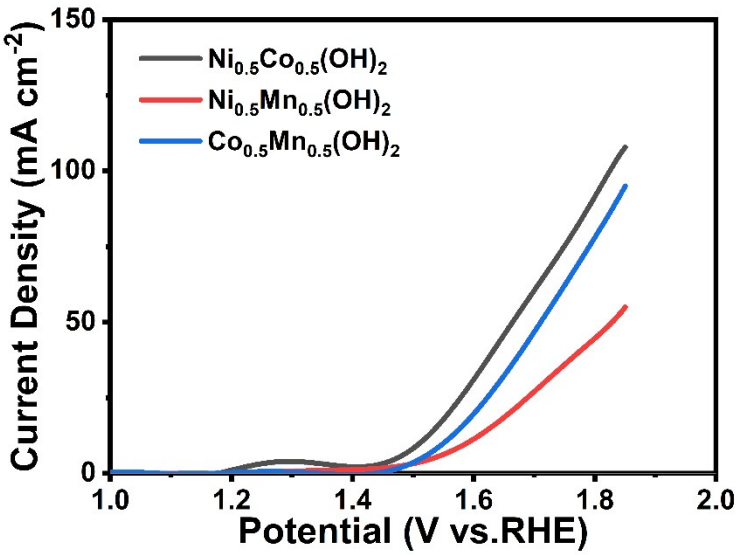

Fig. S5 SCV curves of binary $Ni_{1-x-y}Co_xMn_y(OH)_2$ catalysts in 1.0 M KOH.

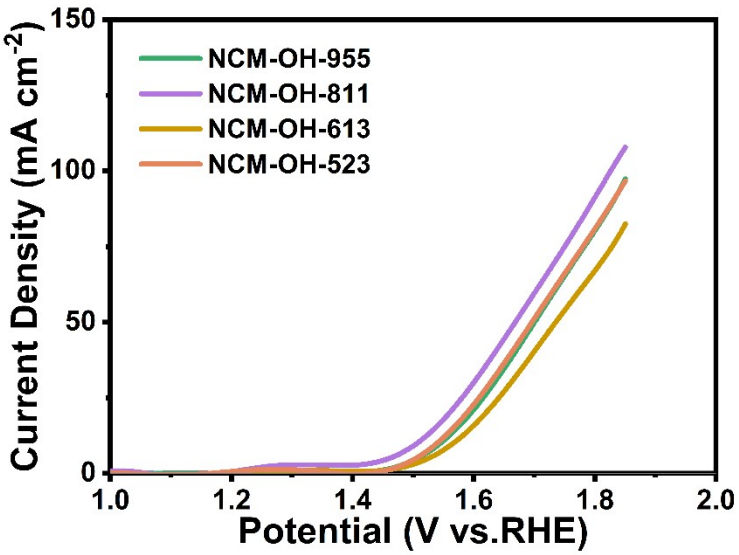

Fig. S6 SCV curves of NCM-OH-(1-x-y)xy catalysts in 1.0 M KOH.

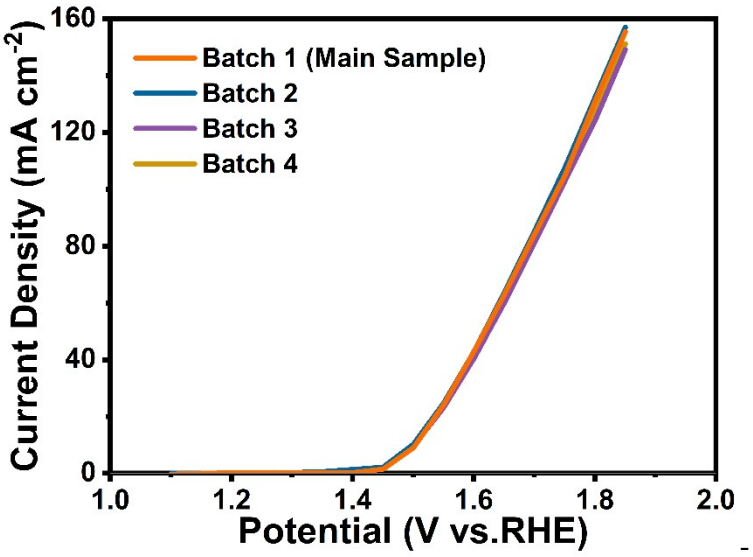

Fig. S7 SCV curves of NCM-OH catalysts made from different batches of spent $LiNi_{0.33}Co_{0.33}Mn_{0.33}O_2$ cathodes. The compositions of the spent cathode materials are slightly different and the details are listed in Table S1. Despite the differences, the SCV curves of as-obtained NCM-OH samples overlap, demonstrating an excellent reproducibility can be maintained within a certain degree of compositional variation.

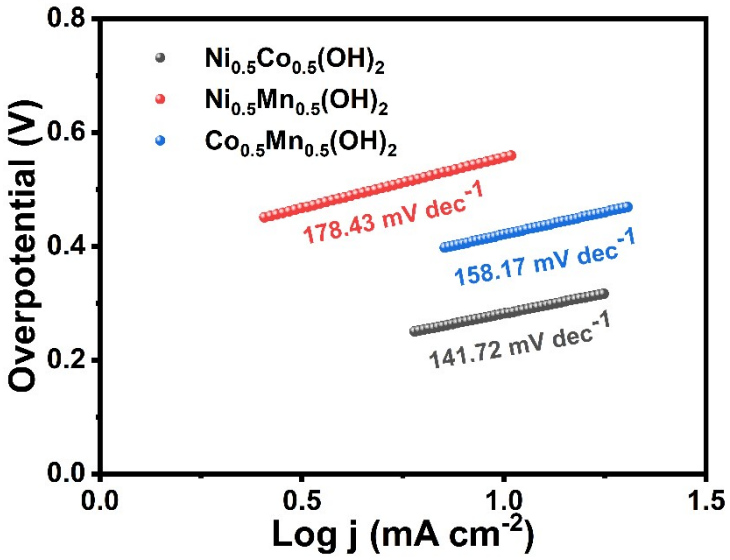

Fig. S8 Tafel slopes of binary $Ni_{1-x-y}Co_xMn_y(OH)_2$ catalysts.

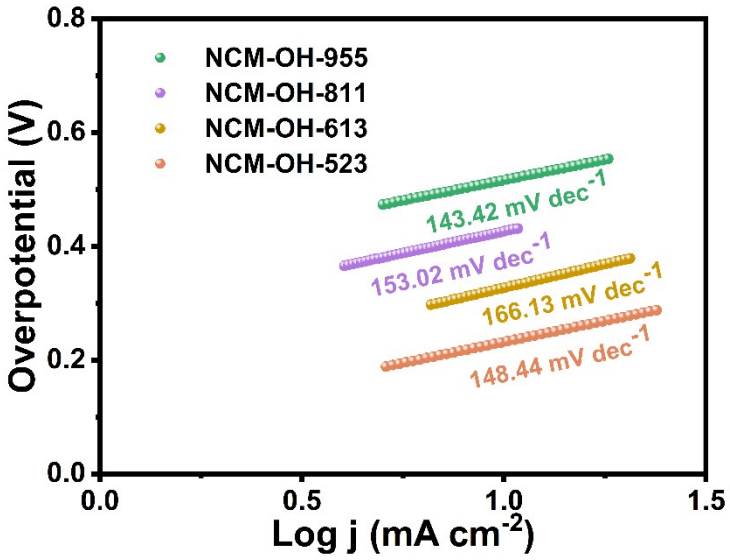

Fig. S9 Tafel slopes of NCM-OH-(1-x-y)xy catalysts.

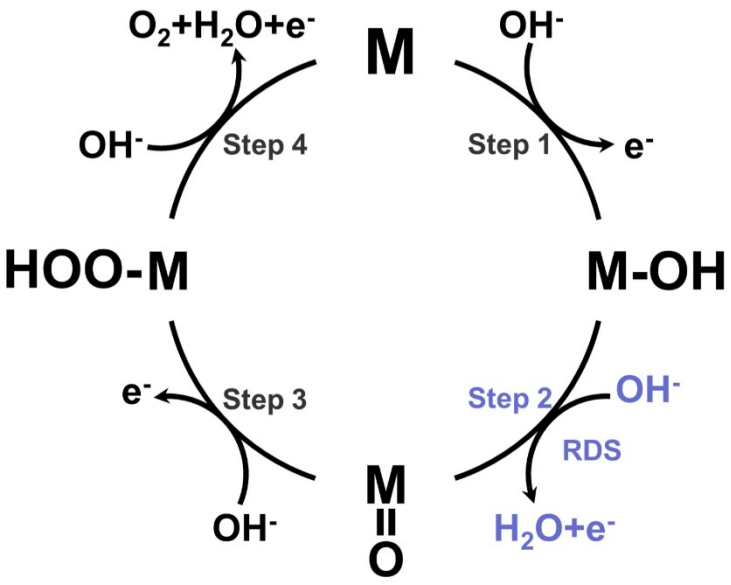

Fig. S10 Proposed mechanism of NCM-OH electrocatalyst for OER.

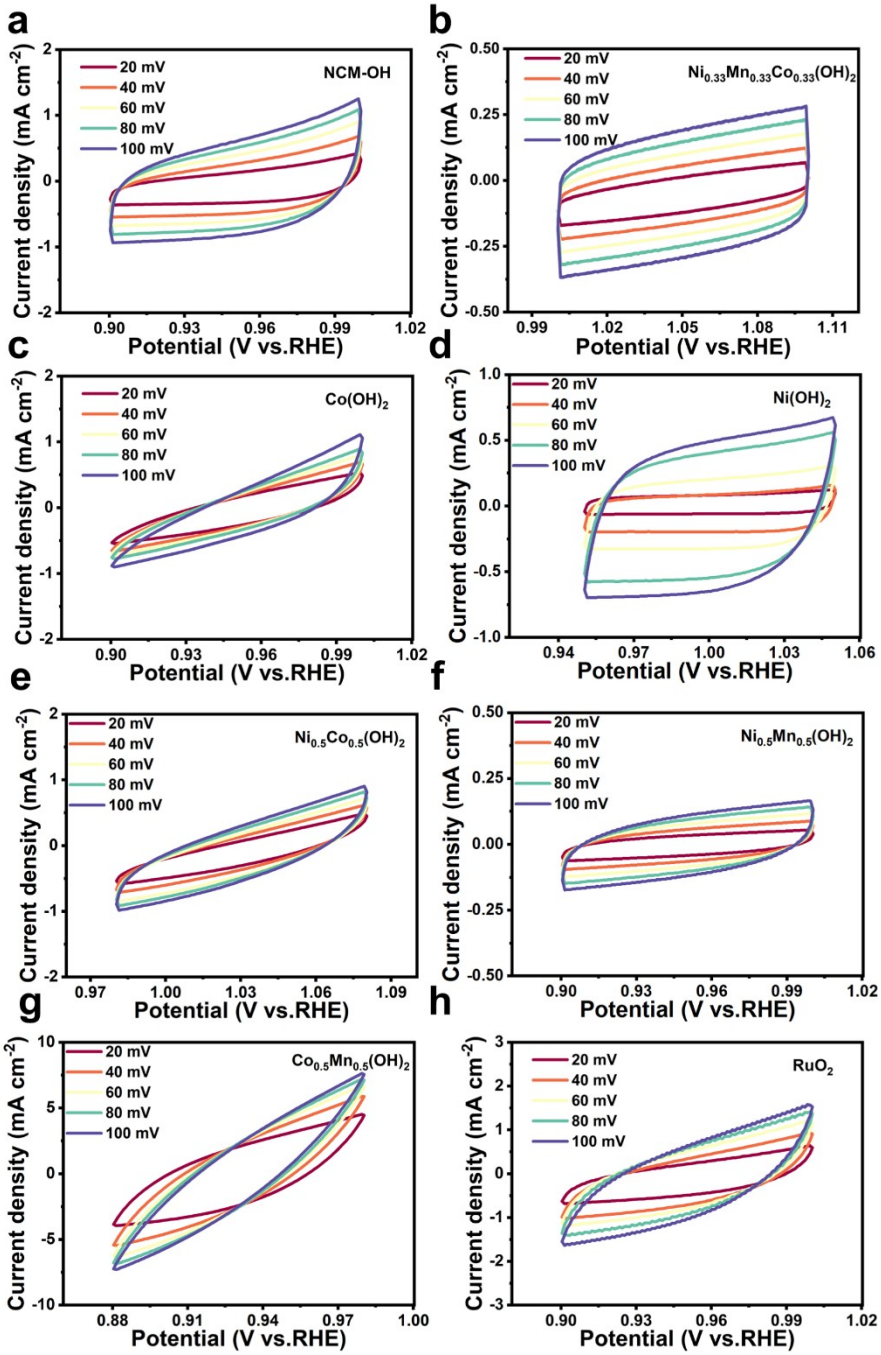

Fig. S11 Electrochemical surface area (ECSA) tests in 1 M KOH. Cyclic voltammetry curves of (a) NCM-OH, (b) $Ni_{0.33}Co_{0.33}Mn_{0.33}(OH)_2$, (c) $Co(OH)_2$, (d) $Ni(OH)_2$, (e) $Ni_{0.5}Co_{0.5}(OH)_2$, (f) $Ni_{0.5}Mn_{0.5}(OH)_2$, (g) $Co_{0.5}Mn_{0.5}(OH)_2$, and (h) RuO_2.

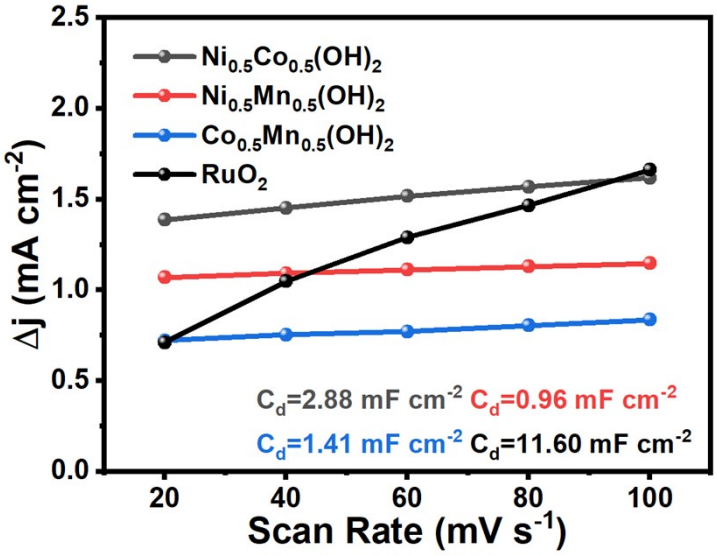

Fig. S12 Double-layer capacitances of different catalysts.

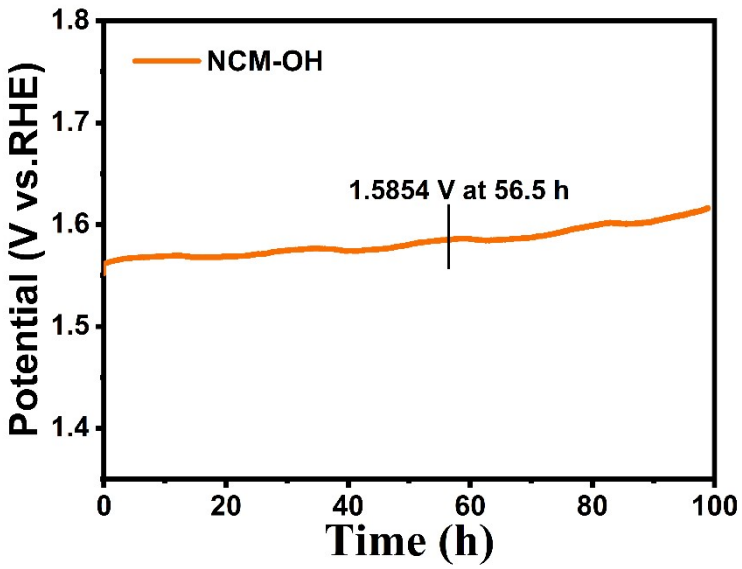

Fig. S13 Chronopotentiometric curve of the NCM-OH catalyst.

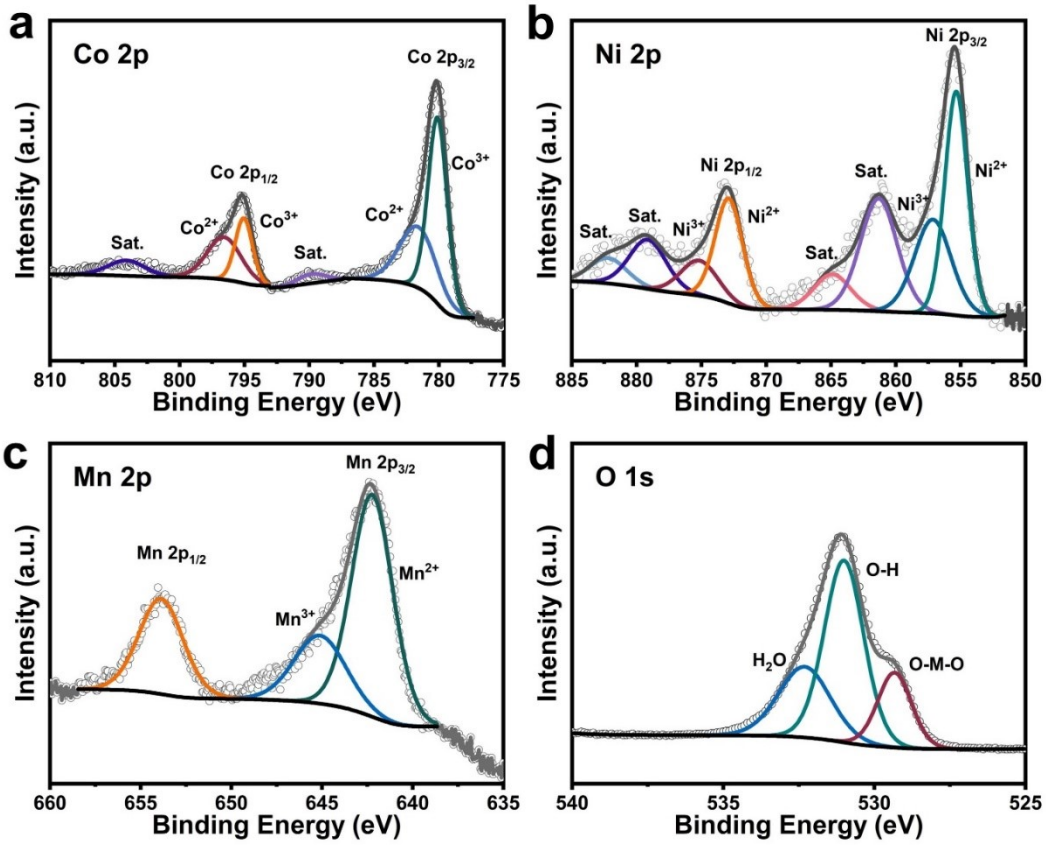

Fig. S14 High-resolution XPS spectra of NCM-OH after CP test.

Table S1. Chemical composition of the spent $LiNi_{0.33}Co_{0.33}Mn_{0.33}O_2$.

Content	Ni	Co	Mn
Batch 1 (Main Sample) (wt.%)	31.15	36.41	32.44
Batch 1 (Main Sample) (at.%)	30.52	35.53	33.95
Batch 2 (wt.%)	33.16	36.62	30.22
Batch 2 (at.%)	32.54	35.79	31.67
Batch 3 (wt.%)	31.77	37.27	30.96
Batch 3 (at.%)	31.16	36.40	32.44
Batch 4 (wt.%)	32.32	37.81	29.87
Batch 4 (at.%)	31.72	36.96	31.32

Table S2. Chemical composition of the NCM-OA.

Content	Ni	Co	Mn
Composition (wt.%)	34.72	37.70	27.58
Composition (at.%)	34.13	36.91	28.96

Table S3. Comparison of the OER performances of our prepared catalysts.

Electrode	Overpotential@10 mA cm^{-2} (mV)	Tafel Slope ($mV\ dec^{-1}$)
NCM-OH	**273**	**50.46**
$Ni(OH)_2$	310	110.23
$Co(OH)_2$	277	84.97
$Mn(OH)_2$	518	291.55
$Ni_{0.5}Co_{0.5}(OH)_2$	279	141.72
$Ni_{0.5}Mn_{0.5}(OH)_2$	356	178.43
$Co_{0.5}Mn_{0.5}(OH)_2$	323	158.17
$Ni_{0.33}Co_{0.33}Mn_{0.33}(OH)_2$	323	127.06
NCM-OH-955	314	143.42
NCM-OH-811	277	153.02
NCM-OH-613	337	166.13
NCM-OH-523	309	148.44
RuO_2	288	80.63

Table S4. Comparison of the OER performance of NCM-OH with recently reported electrocatalysts.

Electrode	Electrolyte	Overpotential @10 mA cm^{-2} (mV)	Tafel Slope (mV dec^{-1})	Life (h/cycles)	Ref.
NCM-OH	**1M KOH**	**273**	**50.46**	**20 h**	**This work**
$Ni_{0.5}Mn_{0.2}Co_{0.3}(OH)_2$	1M KOH	280	6.79	10 h	[1]
NCMB-2	1M KOH	271	57.98	12 h	[2]
Co-O NSs-2nm	1M KOH	288	78	40 h	[3]
NiFe-LDH-V_{Fe}	1M KOH	220	70	2000 cycles	[4]
$Ni_{2.5}Co_5C_2O_4$	1M KOH	330	113	24 h	[5]
$Co_{2.4}Mn_{0.6}O_4$	1M KOH	365	50.6	50 h	[6]
NiCoV-LDH	1M KOH	280	79	16 h	[7]
Sm-$NiMnO_3$	1M KOH	321	109	16 h	[8]
NiMn LDH	1M KOH	310	127	56 h	[9]
MnO_2 NSs/Co_3O_4 NPs-1:2	1M KOH	355	146.3	24 h	[10]
NiFeCo	1M KOH	280	32.25	500 h	[11]
MNC-P/NF 1:1:1	1M KOH	289	85	48 h	[12]

References:

1. Y. Yang, H. Yang, H. Cao, Z. Wang, C. Liu, Y. Sun, H. Zhao, Y. Zhang and Z. Sun, *Journal of Cleaner Production*, 2019, **236**.
2. Z. Chen, W. Zou, R. Zheng, W. Wei, W. Wei, B.-J. Ni and H. Chen, *Green Chemistry*, 2021, **23**, 6538-6547.
3. C. He, L. Yang, X. Peng, S. Liu, J. Wang, C. Dong, D. Du, L. Li, L. Bu and X. Huang, *ACS Nano*, 2023, **17**, 5861-5870.
4. Y. Wang, M. Qiao, Y. Li and S. Wang, *Small*, 2018, **14**, e1800136.
5. S. Ghosh, R. Jana, S. Ganguli, H. R. Inta, G. Tudu, H. Koppisetti, A. Datta and V. Mahalingam, *Nanoscale Adv*, 2021, **3**, 3770-3779.
6. K. R. Park, J. E. Jeon, K. Kim, N. Oh, Y. H. Ko, J. Lee, S. H. Lee, J. H. Ryu, H. Han and S. Mhin, *Applied Surface Science*, 2020, **510**.
7. K. Bera, A. Karmakar, S. Kumaravel, S. Sam Sankar, R. Madhu, N. D. H, S. Nagappan and S. Kundu, *Inorg Chem*, 2022, **61**, 4502-4512.
8. S. Swathi, R. Yuvakkumar, G. Ravi, A. G. Al-Sehemi and D. Velauthapillai, *Nanoscale Adv*, 2022, **4**, 2501-2508.
9. M. Duraivel, S. Nagappan, K. H. Park and K. Prabakar, *ChemElectroChem*, 2022, **9**.
10. G. Yusibova, J.-M. Assafrei, K. Ping, J. Aruväli, P. Paiste, M. Käärik, J. Leis, H.-M. Piirsoo, A. Tamm, A. Kikas, V. Kisand, P. Starkov and N. Kongi, *Journal of Electroanalytical Chemistry*, 2023, **930**.
11. A. I. Inamdar, H. S. Chavan, S. M. Pawar, H. Kim and H. Im, *International Journal of Energy Research*, 2019, **44**, 1789-1797.
12. K. E. Salem, A. A. Saleh, G. E. Khedr, B. S. Shaheen and N. K. Allam, *Energy & Environmental Materials*, 2022, **6**.